Desalination 495 (2020) 114593

Contents lists available at ScienceDirect

Desalination

journal homepage: www.elsevier.com/locate/desal

Potential of supercritical water desalination (SCWD) as zero liquid discharge (ZLD) technology

Surika van Wyk[a,b], Aloijsius G.J. van der Ham[a], Sascha R.A. Kersten[a,*]

[a] Sustainable Process Technology, Faculty of Science and Technology, University of Twente, Postbus 217, 7500 AE Enschede, the Netherlands
[b] Wetsus, European Center of Excellence for Sustainable Water Technology, Oostergoweg 9, 8911 MA Leeuwarden, the Netherlands

ARTICLE INFO

Keywords:
Supercritical water desalination (SCWD)
Zero liquid discharge (ZLD)
Economics
Brine management

ABSTRACT

A modelling and economic study was done to evaluate the suitability of supercritical water desalination (SCWD) as zero liquid discharge (ZLD) technology. ZLD was achieved with a two stage brine treatment process. The hydrothermal brine, remaining after separation of supercritical water (SCW), under supercritical conditions, was expanded in the first stage (flash-step), and the remaining brine was then expanded and dried in the second stage (flash-evaporation step) using the produced steam of the first stage expansion. A window of operation for the first and second stage pressures was determined. For the process, the optimum point of operation was at the maximum second stage pressure, where the exergy of the second stage produced steam was also at a maximum. The economic evaluation showed that the SCWD brine treatment price, for an ideal case where all the products were sold, decreased from $ 9.61 to 1.16/m^3_{brine} when increasing feed concentration from 3.5 to 20 wt% NaCl. The decrease was due to the income from the sale of salts, which increases with feed concentration. The brine treatment price was highly dependent on the brine source and it was recommended that SCWD be used for the treatment of concentrated waste streams.

1. Introduction

Increased brine production and the management of these streams has become a cause for concern. Jones et al. [1] reported the global brine production to be 141.5 million m^3/d. Apart from freshwater production, brine is also produced from other industries including the food and textile industry, petrochemical industry (hydraulic fracturing) and CO_2 sequestration [2,3]. In the United States, the brine production rate of hydraulic fracturing is estimated to be 6.4–8.7 million m^3/d [4]. For CO_2 sequestration, the global brine production rate is projected to be ~31.2 million m^3/d [3,5]. In the past, brine disposal methods included direct discharge into oceans and lakes, deep-well injection and land applications. However, due to growing environmental concerns and revised legislation, alternative methods for the treatment of brine waste are being investigated. Research is focussed on the development of zero liquid discharge (ZLD) technologies, which recovers both salt and water without the production of liquid waste streams [6–8].

Standard reverse osmosis (RO) membranes are favourable for concentrating saline streams up to ~7 wt%, after which the required pressure is too high for the membrane to withstand [7]. Other membrane processes such as electro-dialysis (ED), ultrafiltration (UF), nanofiltration (NF) and high pressure RO are able to achieve higher discharge concentrations [1,6]. Membrane processes alone are not able to achieve ZLD and are usually used in combination with other processes. For more concentrated brine streams (≥7 wt%), thermal desalination techniques, such as multi-stage flash (MSF), multi-effect distillation (MED) and mechanical vapour compression (MVC), are typically used to concentrate the brine up to saturation, after which crystallisation is applied to retrieve the solid salt. The drawback of thermal desalination units is that it becomes more energy intensive as the brine (feed) concentration increases, making the treatment of concentrated waste brines more costly [9,10].

An alternative ZLD desalination technology, for the treatment of brine waste streams, is supercritical water desalination (SCWD). SCWD is the separation of salt and water under supercritical conditions (Temperature > 374 °C, Pressure > 22.1 MPa). Under these conditions the properties of water drastically change, among which is the rapid decrease in the dielectric constant of water (80 to ~5) indicating that the water becomes non-polar [11]. Consequently, inorganic components, such as salts, become insoluble in water and can be easily separated. For NaCl (type I salt), the separation is based on the formation of a pseudo – vapour – liquid equilibrium (VLE) system, where a supercritical water phase (SCW) (vapour), with a low salt concentration, is separated from a concentrated hydrothermal brine phase

* Corresponding author.
E-mail address: s.r.a.kersten@utwente.nl (S.R.A. Kersten).

https://doi.org/10.1016/j.desal.2020.114593
Received 16 March 2020; Received in revised form 15 May 2020; Accepted 15 June 2020

Nomenclature

AP	Anderko & Pitzer
eNRTL	Electrolyte non-random two liquids
ED/EDR	Electro-dialysis (reverse)
EoS	Equation of state
HEX	Heat exchanger
MD	Membrane distillation
MED/MEE	Multi-effects distillation/evaporation
MP	Medium pressure
MSF	Multi-stage flash
MVC	Mechanical vapour compression
NF	Nano-filtration
RO	Reverse osmosis
SC	Supercritical
SCW	Supercritical water
SCWD	Supercritical water desalination
SEE	Single-effect evaporation
SI	Supporting information
TDS	Total dissolved solids
UF	Ultrafiltration
VLE	Vapour liquid equilibrium
ZLD	Zero liquid discharge

Symbols

A	Annualised capital expense
h	Specific enthalpy
Δh_{vap}	Enthalpy of vaporisation
H	Enthalpy of dissociation
i	Interest rate
$\dot{m}$	Mass flow
P	Pressure/Principle value (when indicated)
T	Temperature

Sub-/superscript

opl	Operational
sat	Saturation
sep	Separator/Separation
theo	Theoretical

(liquid) with a high salt concentration [12–14]. This approach to desalination has been tested on both lab-scale [12] and pilot plant scale [13,15,16] for brines (feeds) of varying concentrations (3.5 to 16 wt% NaCl). Depending on the feed concentration and operating conditions, the recovery of drinking water can be up to 93% (mass basis) [13]. The freshwater recovery is higher in comparison to the 50% freshwater recovery (for seawater feeds), achieved by the three most widely applied desalination technologies namely RO, MSF and MED [1,17,18].

Another advantage is that the process becomes less energy intensive with the increase in salt concentration (opposite as for conventional thermal desalination processes). In a recent study on the energy analysis of the SCWD process [19], it was shown that energy consumption of SCWD decreased due to lower heat capacity of the feed stream, which improved the heat exchange potential and reduced the required energy of the heater. It was also shown that energy consumption of the SCWD unit, for concentrated feeds, is comparable with conventional ZLD processes. Studies on SCWD have been mainly focussed on the development and the evaluation of the energy consumption and economics of the SCWD process [12–16,19]. Investigations, into the development of the brine recovery section and further optimisation of ZLD, are limited. For SCWD, ZLD is achieved through the two stage expansion-evaporation of the hydrothermal brine formed in the gravity separator. Preliminary calculations and modelling, showed that ZLD is possible for a first stage expansion pressure of 10 bar and second stage pressure of 1 bar, but detailed modelling and optimisation have not been done [13,16]. With the expansion of the hydrothermal brine, three products are retrieved, namely solid salt, water and steam. By adjusting the ratio between the first and second stage pressure, the steam retrieval and quality could be optimised, while still achieving ZLD. The steam, in turn could be used for pre-heating concentrated feeds to the SCWD, to further reduce the energy consumption of the process, or it could be integrated with other process units [19].

Previously an experimental and modelling analysis was done for the energy consumption of the SCWD unit, specifically looking at the effect of feed concentration on heat exchange potential and heater duty [19]. The study is now extended to the brine treatment section of the SCWD unit. The aim of this work was to model the brine treatment section in more detail, using validated thermodynamic models for the sub – and supercritical region of the process. Additionally, the expansion pressures are optimised, for the production of high-quality steam, while still achieving ZLD. Through modelling and optimisation of the brine expansion section, guidelines can be provided for selecting operating conditions. To our knowledge, this was the first time that the brine expansion section, of the SCWD process, was modelled in detail, investigating the influence of expansion pressures on steam production and providing guidelines for operation in the ZLD region. Afterwards an economic evaluation of the SCWD unit was performed for different feed concentrations to evaluate the economic feasibility of applying the SCWD technique as a ZLD technology. The economic evaluation was done for a more general case (not for a specific waste brine stream) and sensitivity analyses were performed to evaluate the effect of product income, solid disposal and brine inlet temperatures. Lastly, the preliminary brine treatment prices were compared with different desalination, near-ZLD and ZLD processes to evaluate the feasibility of the process.

2. Modelling

2.1. Thermodynamics and validation

The thermodynamic properties of the sub – and supercritical section were modelled using two different models, with the details given in our previous work [19]. The supercritical section was modelled using a Helmholtz free energy based equation of state (EoS) developed by Anderko & Pitzer (AP) [20] for NaCl-H_2O systems. The pure and binary interaction coefficients, reported by Kosinski & Anderko [21] were used for the modelling. The EoS was used for VLE and enthalpy calculations for a temperature range of 300–500 °C, a pressure range of 1–300 bar and concentrations of pure water to concentrated brines (> 50 wt% NaCl).

The subcritical section was modelled using the electrolyte non-random two liquids (eNRTL) activity coefficient model with a symmetric reference state, developed by Song & Chen [22]. The interaction parameters reported by Yan & Chen [23] were used. The subcritical region extends for a temperature range of 20–300 °C, pressures of 1–300 bar and concentrations ranging from pure water to a saturated solution (26 wt% NaCl).

In our previous work [13,19] it was already shown that the AP EoS is able to predict the VLE composition and outlet temperatures of the heat exchanger. In the present contribution, further validation has been done by calculating the product distribution after brine expansion (assuming isenthalpic expansion) and comparing it with the experimental pilot plant results [13]. The ratio of the solid salt to the total salt entering brine expansion section, was also calculated. The calculation

procedure and equations are provided in the supporting information (SI) along with the parity plots for product distribution and solid salt ratio. Overall, the deviation was within ± 15% of the experimental measurements.

2.2. Brine treatment section modelling

From the experimental product distribution obtained in a single stage flash (see SI and [13]), it was seen that along with steam and solid NaCl, water was also produced. This is due to the enthalpy of the brine being insufficient for complete separation between steam and dry NaCl. Previously [13], a two stage flash and flash-evaporator scheme was introduced to illustrate the potential to attain ZLD with our SCWD process. The proposed two step process utilises the steam, obtained from the first flash, in the subsequent flash-evaporation step to dry the salt and produce more steam. This technique is also employed by the commercial MED process. For the process calculations, the evaporator and second stage flash (typically one unit) were modelled separately, according to the scheme shown in Fig. 1.

The calculations for the first and second stage flash, were performed assuming that the expansion was isenthalpic. The steam exiting the first stage flash was at superheated conditions and thus for the evaporator both the sensible and latent heat of the steam (#3) was used to evaporate the water in stream #4-A. The sensible heat of stream #6, was not utilised for drying, thus the temperature of the stream was equal to the saturation temperature of water for the given first stage flash pressure. For some cases, the steam was not fully condensed, resulting in a two phase stream that was further separated into steam (#6-A) and water (#6-B). Both the overall and individual unit, mass and energy balances were checked and closed. The detailed mass and energy balance equations of the system are given in the SI.

2.2.1. ZLD operation pressures and steam production

For the above system, only the first and second stage pressures are set. In previous studies [13,16], the first and second stage pressure was set to 10 and 1 bar respectively, to illustrate the possibility of achieving ZLD with SCWD. However, the ratio between the two pressures can be varied, to achieve ZLD and to optimise steam production and quality (stream #5 and #7 - Fig. 1).

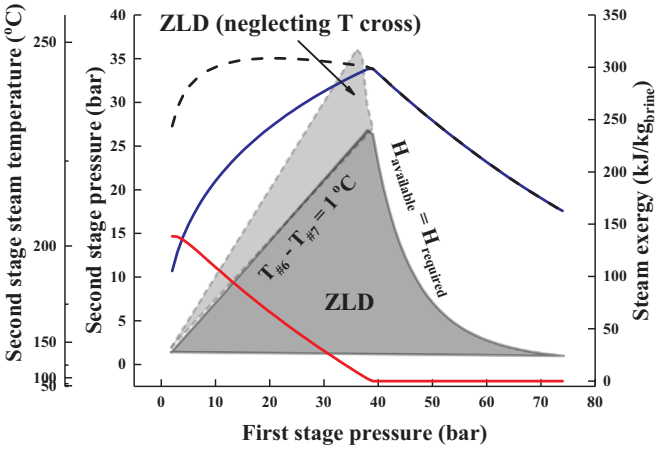

Fig. 2. ZLD operating window of brine treatment section and steam exergy for T_{sep} = 430 °C, P_{sep} = 270 bar and x_{NaCl} = 38 wt% (■ ZLD area neglecting evaporator temperature cross; ■ ZLD area considering evaporator temperature cross; ■ Exergy stream #5 + #7 (at second stage pressure); ■ Exergy stream #6 (at first stage pressure); ■ (dashed line) Total steam exergy (#5 + 7 + 6)).

The maximum second stage pressures for which ZLD can be achieved was determined for selected first stage pressures, from the mass and energy balances of the brine treatment section (see SI). In this manner a window of operation, in which the brine treatment section can operate to achieve ZLD, was drawn.

The operating pressures were solved for a hydrothermal brine entering at 430 °C and 270 bar, with a NaCl concentration of 38 wt%. In Fig. 2, the resulting ZLD operating window is presented along with the exergy of the first (stream #6) and second (stream #5 + 7) stage produced steam and the total steam exergy. The operating window can be divided into two sections. The first section starts on the left-hand side and reaches up to the maximum second stage pressure of the dark grey ZLD area. For this section, a surplus amount of energy (from the

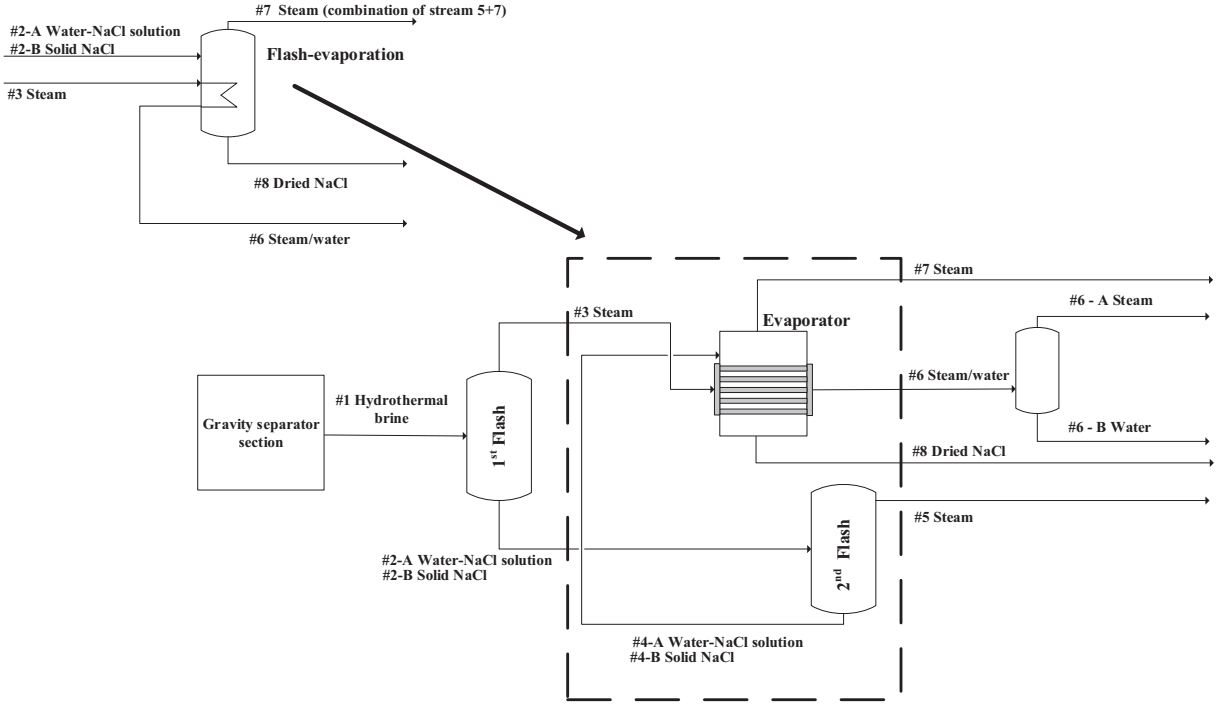

Fig. 1. Two step flash-evaporation scheme for ZLD (adapted from [13]).

first stage expansion) is available for drying the salt in the evaporator. Consequently, a temperature cross would occur inside the evaporator. Two second stage pressure boundary lines are drawn in this section of the operating window. The first line (light grey dashed line – boundary of the light grey ZLD area), ignores the temperature cross inside the evaporator (neglects the second law of thermodynamics) and the first and second stage pressures, are equal as a sufficient amount of energy is available for drying. The second line (solid line - boundary of the dark grey ZLD area), considers the temperature cross inside evaporator and the second stage pressure was solved for a temperature difference of 1 °C (between $T_{\#6}$ and $T_{\#7}$). The corresponding steam temperature for the second stage pressure can be read from the most left-hand side axis (the axis is scaled to correspond with the second stage pressure axis). The steam (both the first and second stage) is at superheated conditions and not at saturation, due to the presence of the salts that increase the expansion temperature (boiling point elevation effect). For example, for a first stage pressure of 10 bar, the second stage pressure, neglecting the temperature cross inside the evaporator, would also be 10 bar and the steam temperature 194 °C. If the temperature cross is considered, the second stage pressure would be 7.0 bar and the steam temperature 178 °C.

The second section of the operating window starts at the maximum second stage pressure (of the dark grey ZLD area) and stretches to the right-hand side of the operating window. For this section, the amount of energy available for drying the salt in the evaporator becomes limited.

The second stage pressure boundary (dark grey ZLD area) was drawn, assuming that the steam (stream #3) was fully condensed (at first stage pressure) inside the evaporator. The enthalpy available for drying ($H_{availble}$) is the sum of the sensible and latent heat of the superheated first stage steam and was set equal to the enthalpy required ($H_{required}$) for drying the salt.

$$\Delta H = H_{availble} - H_{required} \tag{1}$$

With:

$$H_{available} = \dot{m}_3 h_3 (T_{flash,1}, P_{flash,1} \rightarrow T_{sat}, P_{flash,1}) + \dot{m}_3 \Delta h_{vap} (P_{flash,1}) \tag{2}$$

$$H_{required} = (\dot{m}_7 h_7 + \dot{m}_8 h_8) - (\dot{m}_{4A} h_{4A} + \dot{m}_{4B} h_{4B}) \tag{3}$$

For $\Delta H > 0$, a surplus amount of energy is available and stream #6 will contain some steam, while for $\Delta H < 0$, ZLD will not be achieved and a brine will be produced in stream #8. The second stage pressure was solved for $\Delta H = 0$.

The above description covers the drawing of the ZLD operating window. Next to evaluate the steam quality, the exergy of the steam was calculated (see SI) for the remaining steam in stream #6 (at first stage pressure) and stream #5 + 7 (at second stage pressure). The total exergy (stream #6 + #5 + #7) was also drawn. The exergy was normalised for the amount of hydrothermal brine (stream #1 = 0.9 kg/h) fed to the brine treatment unit and the curves were drawn at the boundary conditions of the ZLD area (dark grey area). For example, for a first stage pressure of 10 bar, the exergy of stream #6 (red line – Fig. 2) is 109 kJ/$kg_{brine.}$ The exergy of the stream #5 + 7 (blue line – Fig. 2) is 191 kJ/kg_{brine}, the pressure of the steam is 7.0 bar and the corresponding steam temperature is 178 °C. For the first section of the operating window, (left-hand side until the maximum second stage pressure) three different exergy lines are observed, for stream #6, stream #5 + 7 and the total. For the second section of the operating window (from the maximum second stage pressure to the right-hand side), stream #3 was fully condensed and the exergy of stream #6 was zero as there was no residual steam left. The total exergy was thus equal to the exergy of stream #5 + 7.

Upon examining Fig. 2, it is seen that the second stage pressure (dark grey ZLD boundary curve) increases until a maximum of 26.7 bar (corresponding first stage pressure is 38 bar). After this point, the amount of energy available for drying the salt in the evaporator becomes limited and the second stage pressure starts to decrease. The second stage pressure decreases, so that more steam will be formed (the content of stream #5 will increase) during the second stage expansion and thus less energy will be required to evaporate the remaining water and dry the salt. As mentioned, the steam exergy curves were drawn as a measure of the quality of the steam produced. The ideal operating point would lie at the maximum exergy point, as the maximum amount of useful work can be extracted. For the total exergy, it is seen that between a first stage pressure of 10 and 38 bar, the total exergy remains relatively constant. Between these pressures, the exergy of stream #5 + 7 continues to increase, due to the increase in the second stage pressure. The exergy of stream #6 decreases, due to a decrease in the vapour content. The exergy of stream #5 + 7 reaches a maximum point around the maximum second stage pressure (the exergy of stream #6 will become zero at this point) and then starts to decrease again. The decrease of the exergy is due the loss in mechanical work potential, with the second stage expansion. If, for example, a horizontal line is drawn for a second stage pressure of 5 bar, the two first stage boundary pressures are 7 and 53 bar. For 7 bar, the pressure drop would be 2 bar, while for 53 bar the pressure drop would be 48 bar, which translates into a greater loss of potential mechanical work.

In order to detail the influence of the pressure, the effect of the first and second stage pressure on the steam exergy, is shown in Fig. 3. For Fig. 3a, the first stage pressure was kept constant at 30 bar and the second stage pressure was varied between 2 and 21 bar (pressure range in the dark grey ZLD area – Fig. 2). In Fig. 3b, the second stage pressure

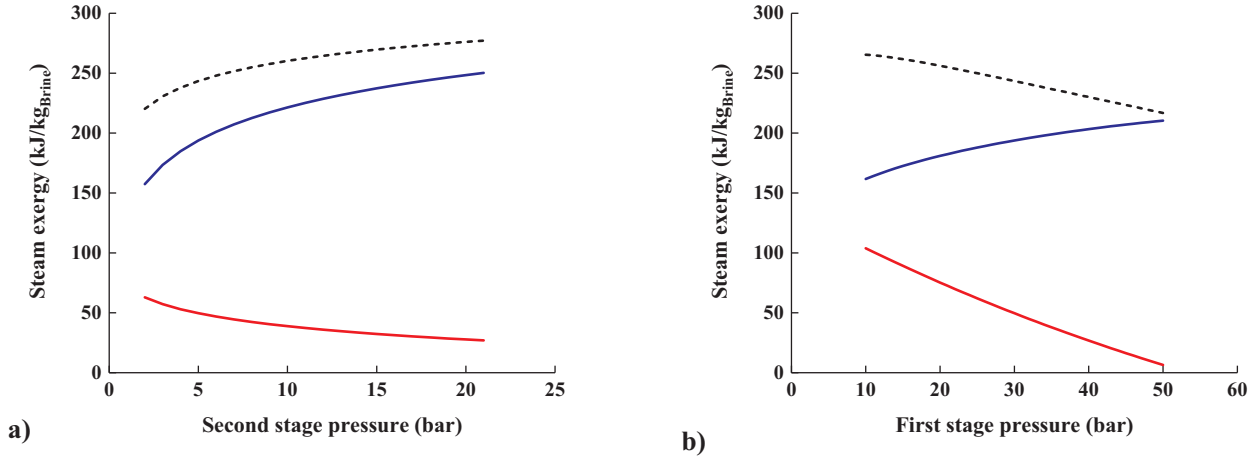

Fig. 3. Effect of first and second stage pressure on the steam exergy a) Constant first stage pressure at 30 bar b) Constant second stage pressure at 5 bar (■ Exergy stream #5 + #7 (at second stage pressure); ■ Exergy stream #6 (at first stage pressure); ■ (dashed line) Total steam exergy (#5 + 7 + 6)).

was kept constant at 5 bar and the first stage pressure was varied between 10 and 50 bar.

From Fig. 3a, it is seen that the exergy of both the first (stream #6) and second stage (stream #5 + 7) steam is affected by the second stage pressure. The exergy of stream #5 + 7 increases, due to the increase in second stage pressure and temperature (quality of steam increases). Conversely, the exergy of stream #6 decreases as the energy required, for evaporating the water in the second stage evaporator, increases (water content of second stage brine increases with pressure). The remaining vapour content of stream #6 decreases and thereby the exergy. The total exergy increases with second stage pressure, which is due to the increase in the exergy of stream #5 + 7.

From Fig. 3b, it is seen that the exergy of steam #5 + 7 increases with first stage pressure, which is caused by the increase in the water content of the brine (stream #2-A) fed to the second stage flash-evaporator (the amount of evaporated steam increases). The exergy of stream #6, in turn decreases due to the decrease in the steam content of the first stage flash, with pressure. The result is that the total exergy also decreases with first stage pressure, until it becomes equal to the exergy of stream #5 + 7 (the exergy of stream #6 becomes zero and the stream is fully condensed).

Returning to Fig. 2, from an operational point of view, it would be best to always operate on the left-hand side of the curve to avoid the loss of potential work. For the purpose of this study, an operating point was selected where the steam content and quality of stream (#5 + 7) was sufficient to pre-heat the concentrated feeds (14 and 20 wt%) entering the SCWD unit. At the maximum exergy of stream #5 + 7, both the quality (26 bar and 245 °C) and content of the steam was sufficient for pre-heating concentrated feeds. At this point the exergy of stream #6 was zero, so there was no loss of potential work in the stream.

2.2.2. *Effect of separation temperature and pressure*

The effect of separation temperature and pressure (stream #1 - different hydrothermal brine concentrations) on the expansion pressures and steam production was investigated. The results for varying separation (hydrothermal brine feed) temperatures (420–450 °C), for a constant pressure of 270 bar are shown in Fig. 4. Only the steam exergy of stream #5 + 7 (for the solved second stage boundary of the dark grey ZLD operating window) is reported, as this stream is used for pre-heating the concentrated feed.

For Fig. 4a, the second stage pressure curves were drawn for the same constrains as the dark grey ZLD area of Fig. 2. For the left-hand side of the operating window (until the respective maximum second stage pressures), the second stage pressure is the same for all concentrations, as there is a surplus amount of energy available in all cases and the second stage pressure is solved for a temperature difference of 1 °C inside the evaporator. The maximum pressure increases with the hydrothermal brine concentration. The increase in maximum pressure is related to the increase in the ratio of the first stage steam to water content $\left(\frac{m_{\#3}}{m_{\#2A,water}}\right)$, with separation temperature (see Fig. 4b). For a higher separation temperature, more steam is produced relative to water and more energy is available for drying the salt in the evaporator. For a pure water system, the maximum second stage pressure would be located at a first stage pressure where the ratio of steam to water is equal to one $\left(\frac{m_{\#3}}{m_{\#2A,water}} = 1\right)$. However, due to the presence of salts, more energy is required to evaporate the water and the ratio of steam to water has to be greater than one. For the above system, it is seen that for a first stage pressure where the ratio of steam to water is ± 1.02 $\left(\frac{m_{\#3}}{m_{\#2A,water}} \sim 1.02\right)$, the corresponding second stage pressure will be at the maximum (see Fig. 4b). This ratio is applicable for a selected evaporator temperature difference of 1 °C, for higher temperature differences the ratio will be higher.

Furthermore, it is seen from Fig. 4a, that the steam exergy decreases with separation temperature. This is due to the increase in the brine salt concentration, which results in a lower steam content. After the respective maximum second stage pressures, the exergies of the steam decrease rapidly due to the loss of potential mechanical work. Operating at a lower separation temperature (lower brine concentration) appears to be advantageous for steam production, however, there would be drawbacks with regards to the SCW quality and recovery in the upstream separator. The amount of salt retrieved after expansion will also decrease, which is disadvantageous for the economic feasibility of the process (see Section 3).

The effect of separation pressure (stream #1) was investigated for a range of 250 to 300 bar, at a constant separation temperature of 430 °C. The results can be seen in Fig. 5.

For varying separation pressures, it is once again seen that the second stage pressure remains constant for the first part of the operating window (surplus energy is available). The maximum pressure increases, again due to the increase in the first stage steam to water ratio (Fig. 5b). This is similar to what was seen for different separation temperatures and is due to the increase in the specific enthalpy of brine (due to lower salt concentration). Once more the maximum second stage pressure is located at a first stage pressure for which the ratio of steam to water is ± 1.02 (see Fig. 5b).

For higher separation pressures, the amount of brine increases, while the brine concentration decreases. With regards to the steam exergy, it is seen that the exergy increases with separation pressure, due to the lower salt concentration of the brine and also the higher second

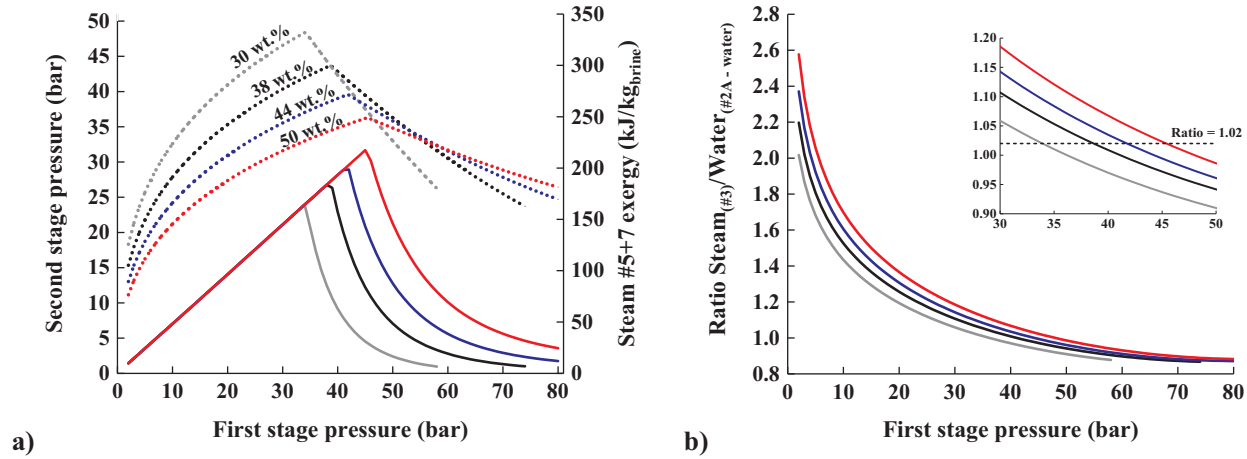

Fig. 4. Effect of separation temperature at 270 bar a) on the ZLD window of operation (solid line) and steam exergy of stream #5 + #7 (dashed line; hydrothermal brine inlet concentrations reported) b) Ratio of first stage steam to water content (■ 420 °C; ■ 430 °C; ■ 440 °C; ■ 450 °C).

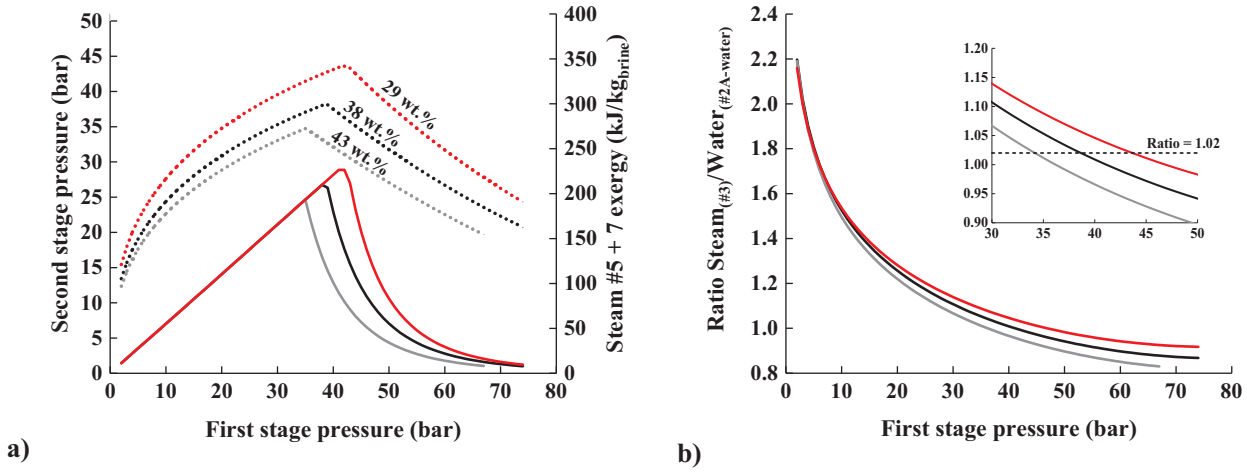

Fig. 5. Effect of separation (brine feed) pressure at 430 °C a) on the ZLD window of operation (solid line) and steam exergy (dashed line; inlet brine concentrations reported) b) Ratio of first stage steam to water content (■ 250 bar; ■ 270 bar; ■ 300 bar).

stage pressures (holds for the second part of the ZLD operating window).

2.2.3. Maximum operating pressures

Determining the maximum pressures of the ZLD operating window (for the given hydrothermal brine inlet conditions) provides a first estimation for the possible operating pressures. From Section 2.2.1 it was recommended to operate near the maximum second stage pressure, as the least amount of potential work is lost in this area (steam exergy was at a maximum).

From Fig. 2, it was seen that there are two maximum pressures for which ZLD can be achieved; the theoretical and the operational maximum. For the theoretical maximum, the temperature cross inside the evaporator is neglected, while for the operational maximum the temperature cross is considered.

Both the theoretical and operational (see Section 2.2.2) maximum pressures depend on the amount of energy available for drying, which in turn depends on the hydrothermal brine inlet conditions. The maximum theoretical point lies where the first and second stage pressures are equal $\left(\frac{P_2}{P_1} = 1\right)$ and the energy available for drying is equal to the energy required for drying (without expansion in the second stage). The theoretical pressures can thus be determined by equating the pressures and solving the mass and energy balance for $\Delta H = 0$ (see Eq. (1)).

In addition to the hydrothermal brine inlet conditions, the maximum operational pressures are dependent on the selected temperature difference inside the evaporator. The operational maximum pressure lies at the point where 1) the process becomes limited by the energy available for drying the salts and 2) the temperature difference inside the evaporator is equal to the specified temperature difference. For the operational maximum, the second stage pressure is always lower than the corresponding first stage pressure $\left(\frac{P_2}{P_1} < 1\right)$. For calculating the operational pressures, the same procedure, as described in Section 2.2.1, would have to be followed (Fig. 2 – dark grey ZLD area). The first stage pressure has to be varied for a certain range and the corresponding second stage pressure has to be calculated for the selected temperature difference inside the evaporator. From the calculated pressures, the maximum second stage pressure can then be identified. Calculating the operational pressures is thus more tedious. However, calculating the maximum theoretical pressures can already provide a good estimate of the operating area. In Table 1, the calculated theoretical and operational maximum second stage pressures and corresponding first stage pressures are given, for different hydrothermal brine conditions and selected temperature differences inside the evaporator.

From the results the following observations can be made regarding the relationship between the theoretical and operational maximum points. Firstly, the theoretical first stage pressure of the maximum point will always be lower than the operational first stage pressure ($P_{1,\ theo} < P_{1,\ opl}$). Secondly, the maximum theoretical second stage pressure will also be higher than the maximum operational second stage pressure ($P_{2,\ theo} > P_{2,\ opl}$). These two observations provide guidelines for selecting possible operating pressures from the determined theoretical maximum. Furthermore, it is seen that the operational first stage pressure is not greatly affected by the selected temperature difference (increased with 2 bar), however, the operational second stage pressure decreased with 7 bar.

2.2.4. Steam integration and SCWD energy consumption

In Fig. 6, the second stage steam (stream #5 + #7) exergy for different feed concentrations is given. In this case, the steam exergy was normalised with respect to the feed rate of the entire SCWD unit, which is 10 kg/h for all concentrations.

Table 1
Theoretical and operational maximum pressures of the ZLD operating window for different conditions.

Temperature (°C)	Pressure (bar)	Brine concentration[a] (wt% NaCl)	Temperature difference (°C)	Theoretical pressure (bar)	Operational first stage pressure (bar)	Operational second stage pressure (bar)
420	270	30	1	33	34	24
430	270	38	1	35	38	27
430	270	38	20	35	40	20
430	250	43	1	33	35	25
430	300	29	1	41 (40.5)	41	29
440	270	44	1	39	42	29
450	270	50	1	42	45	32

[a] Refers to the hydrothermal brine concentration entering the first stage flash.

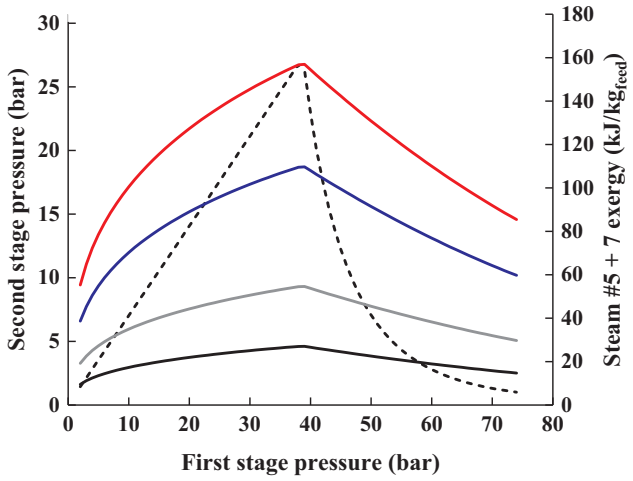

Fig. 6. Effect of feed concentration at 430 °C and 270 bar (dashed line – second stage pressure, solid line – steam exergy (#5 + #7); ■ 3.5 wt%; ■ 7 wt%; ■ 14 wt%; ■ 20 wt%).

The second stage pressure remained the same for all concentrations as the brine concentration and the selected evaporator temperature difference was constant. For higher concentration feeds, more steam was retrieved due to the increase in brine content with feed concentration.

From our previous work [19], it was shown that pre-heating of higher concentration feeds (14 and 20 wt%) would improve the heat transfer potential in the SCW-Feed heat exchanger (supercritical (SC) -HEX, see Fig. 7). Calculations showed that pre-heating a 20 wt% NaCl feed to 200 °C, would require 0.56 MJ_{th}/kg_{feed}, of which 70% could be provided by the SCW stream, through stream splitting [19]. The remaining 0.17 MJ_{th}/kg_{feed} would have to be provided by medium pressure (MP) steam (20 bar; 220 °C). However, with the above ZLD scheme, the remaining energy can be easily provided by the produced second stage steam rather than a utility stream. At the maximum steam exergy point (steam pressures is 26.32 bar) the total latent heat of the steam for a 20 wt% feed, is 2.78 MJ_{th}/h (feed of 10 kg/h), which is sufficient for heating the feed stream from 25 to 200 °C (1.7 MJ_{th}/h is required after stream splitting). Similarly, for a 14 wt% feed, the produced steam could be used to pre-heat the stream to 100 °C. This in turn reduces the operational costs of the unit. In Table 2, the updated summary of the total SCWD energy consumption is given. For the detailed explanation on the calculation of the SCWD energy consumption, the reader is referred to our previous work [19]. The pump and feed heater duty, for a feed of 3.5 and 7.0 wt%, remained the same as previously reported. For a feed of 14 and 20 wt%, pre-heating was required to compensate for the fact that the SCW recovery decreases with higher feed concentrations, which alters the heat exchange potential inside the SC HEX (see Fig. 7). Previously pre-heating was done using external steam. External pre-heating is no longer required as the steam can be retrieved from the brine treatment unit and the energy consumption decreased. The decrease was 4% for a feed of 14 wt% and 24% for a feed of 20 wt%. The overall energy consumption was also normalised for the amount of salt fed to the SCWD unit, to show that the process becomes less energy intensive as the salt concentration of the feed increases. The NaCl cooling duty, required to cool the dried NaCl existing the unit, was also included. In Table 2, the cooling requirement for a stream cooled from 245 (26 bar) to 50 °C, using cooling water (assume a cooling water temperature increase of 10 °C), is reported.

3. Economic evaluation

An economic analysis was performed to give an indication of the cost of the proposed SCWD unit as shown in Fig. 7. The feed stream splitting section, shown in Fig. 7, is only applicable for higher concentration feeds (14 and 20 wt%).

The capacity of conventional desalination plants varies greatly, depending on the region and the type of technology. Capacities range from small scale plants of 1000 m^3/d to larger plants with a capacity of more than 250,000 m^3/d [1,24]. Thermal desalination plants have smaller capacities ranging from 5000 to 15,000 m^3/d for MED and 50,000–70,000 m^3/d for MSF. RO plants have capacities up to 250,000 m^3/d [1,25]. The economy-of-scale is observed for desalination plants up to certain capacities. For thermal desalination plants with high salinity feeds, the optimum capacity is ≥25,000 m^3/d for MSF and between 10,000 and 25,000 m^3/d for MED [1]. The freshwater recovery (for a seawater feed) varies, but is usually less than 50% [1]. For the economic analysis, the SCWD was regarded as a post-treatment unit for the treatment of concentrated brine waste (*e.g.* produced during desalination). For the preliminary evaluation, the size/capacity and cost of the SC HEX and SC Heater was considered (see Fig. 7). The SC HEX was designed as a multiple-tube, hairpin HEX, operated in pure counter-current flow and able to withstand high operating pressures and temperatures. The approximate surface areas for these units are 10–200 m^2 [26]. The surface area of the SC HEX was determined using the U.A/m_{feed} value of 20 kJ/kg.K and assuming an overall heat transfer coefficient of 1500 $W/m^2.K$ [12,19]. The SC heater was chosen to be a box type furnace (fired heater), with capacities ranging from 10 to 340 million Btu/h (3–100 MW) [27]. The duty for the SC Heater was calculated using the calculated heater duties (in MJ_{th}/kg_{feed}) from Table 2, for the different concentrations and feed rates. The required size/duty of each unit was then divided by the amount of brine fed, to get the unit size per capacity brine. This value was then used to determine the maximum capacity of the units. The results are presented in Table 3.

Table 2
SCWD energy consumption (adapted from [19]).

Feed concentration (wt %)	Pump duty[a] (MJ_{th}/kg_{feed})	Feed heater inlet temperature[h] (°C)	Feed heater duty[h] (MJ_{th}/kg_{feed})	Overall energy consumption[b] (MJ_{th}/kg_{feed})	Overall energy consumption[b] (MJ_{th}/kg_{salt})	NaCl cooling requirement[c] (MJ_{th}/kg_{feed})
3.5	0.048	389	0.81	0.90	26	0.006
7.0	0.046	390	0.78	0.93	13	0.012
14[d]	0.042	385	0.70	0.74 (0.77)[f]	5.3	0.025
20[e]	0.039	397	0.50	0.54 (0.71)[f]	2.5	0.035

[a] Thermal energy requirement (50% efficiency).
[b] Sum of thermal energy of pump and feed heater.
[c] NaCl is cooled from 245 to 50 °C.
[d] Pre-heated to 100 °C.
[e] Pre-heated to 200 °C.
[f] Original energy consumption [19] given in brackets.
[h] Feed heater refers to the SC Heater shown in Fig. 7.

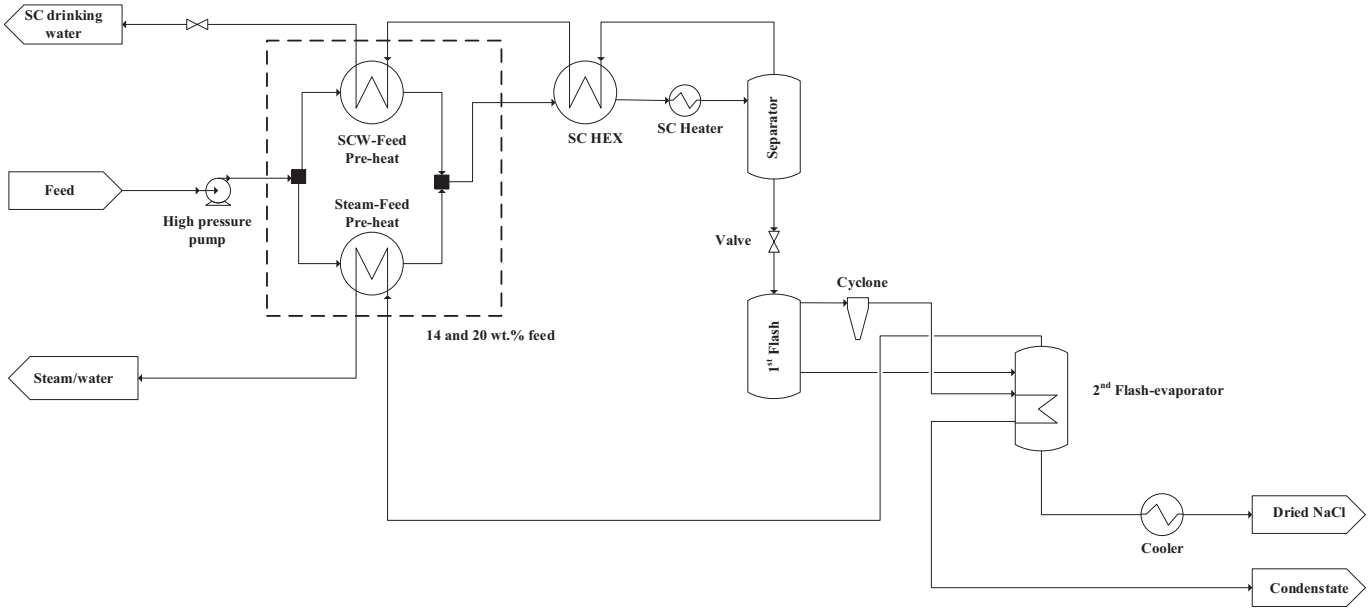

Fig. 7. SCWD with ZLD & heat integration.

Table 3
Required unit size (SC HEX and SC Heater) and maximum capacity for different feed concentrations.

Feed concentration (wt%)	SC HEX size $\left(\frac{m^2_{HEX\ area}}{m^3_{Brine}/d}\right)$	SC HEX maximum capacity[a] (m^3/d)	SC Heater size $\left(\frac{MW}{m^3_{Brine}/d}\right)$	SC Heater maximum capacity[b] (m^3/d)
3.5	0.158	1266	0.0097	10,300
7.0	0.161	1242	0.0094	10,600
14	0.170	1176	0.0089	11,250
20	0.177	1130	0.0067	15,000

[a] Maximum area of 200 m^2.
[b] Maximum duty 100 MW.

The results show that the maximum capacity, for a single SC HEX, is ± 10 times lower in comparison to the maximum capacity for the SC Heater, with values for the SC Heater reaching up to 15,000 m^3/d for concentrated feeds. A fired heater is considerably more expensive than a HEX, due to the design and materials. Installing multiple HEXs would therefore not be as costly compared to a single fired heater. For further consideration of the plant capacity, the cost and size of the downstream gravity separator was also calculated. The separator is a pressure vessel (designed to withstand pressures of 300 bar), made of special corrosion resistant material (Incoloy 825). Vertical pressure vessels have a maximum weight of 455 tons [27]. In Fig. 8, the cost per capacity of multiple HEXs, a fired heater and the one or more separators are compared for a feed of 3.5 wt% NaCl (most extreme case since it will require the largest units). The material of construction was Ni alloy for the HEX tubing and Incalloy for the tubes in the fired heater. Incoloy 825 was selected for the separator.

From the results it is seen that the cost of multiple HEXs and separators are less than the cost of a single fired heater. From 500 to 5000 m^3/d, the cost of the separator increases due to the size and wall thickness of the vessel increasing for a higher capacity. From a capacity of 5000 to 10,000 m^3/d the size of the vessel remains the same, but two vessels would have to be installed. The cost per capacity will thus remain the same. Furthermore, it is seen that the biggest decrease in cost, for the fired heater and HEXs, is from a capacity of 500 to 5000 m^3/d. From 5000 to 10,000 m^3/d, the equipment cost remained almost constant for the separators and HEXs, while for the heater it decreased marginally. A further increase in the capacity of the SCWD process would thus not benefit the cost of the units. For the economic evaluation, the chosen capacity is 5000 m^3_{feed}/d and it can be viewed as a post-treatment step for a MED plant or a small-scale RO plant.

3.1. Capital investment

The economic analysis was done for a SCWD unit with a feed rate of 5000 m^3/d and an availability of 330 days per year. The feed concentration was varied for 3.5, 7, 14 and 20 wt% NaCl and the separation temperature and pressure were fixed at 430 °C and 270 bar. The first and second stage expansion pressure was set to 40 and 22 bar respectively, for optimum steam production, while still achieving ZLD. 40 and 22 bar were selected as the expansion pressures, so that the temperature difference inside the second stage evaporator was 15 °C. At the maximum second stage steam exergy point ($P_{1st\ stage}$ – 39 bar and $P_{2nd\ stage}$ – 26 bar) the temperature difference was only 3.5 °C, meaning that the evaporator surface area would have to be large. For 40 and 22 bar, the

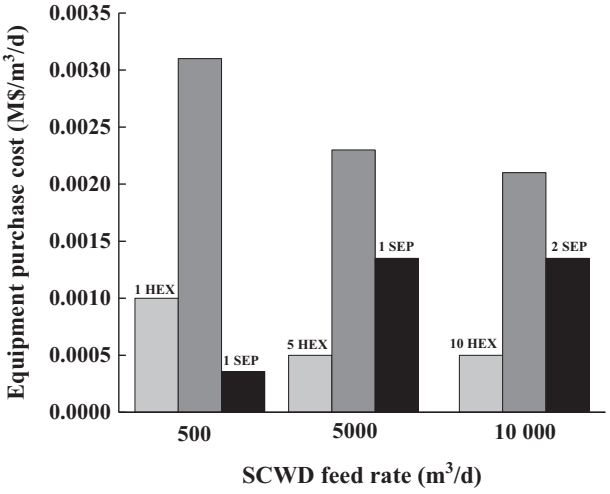

Fig. 8. Comparison of the purchase cost per capacity of multiple tube hairpin heat exchangers, fired heater and gravity separator costs – 2018 for three SCWD feed flows (■ – HEX (Area of 1 HEX = 200 m^2); ■ – Fired heater; ■ – Gravity separator (SEP)).

surface area was smaller and the steam produced was still sufficient for pre-heating concentrated feeds.

The annual feed rates and production flows are given in Table 4. All mass and energy balances were performed using the models and equations given in SI (Section S.1) and [19]. A complete stream table for a 20 wt% feed is given in the SI.

The capital investment was estimated according to the overall factor method of Lang [27]. The total bare module cost of the equipment was multiplied with a factor 4.28 (Lang factor for fluids-solids processing plant) to obtain the total fixed capital investment, within an accuracy of ± 35%. The year basis for the capital cost was 2018 (chemical engineering index = 603.1 [28]) and costing was done in US dollars. The major equipment sizing and costing was done according to the methods described in Seider et al. [27], Peters et al. [26] and Woods [29], with further details provided in the SI. In Table 5 a summary is given of the purchase costs, material of construction, and design pressure and temperatures, as well as the final fixed capital investment.

Only the major equipment was considered for the capital investment. As mentioned in Section 3, the SC HEX, SC heater and separator were constructed from corrosion resistant materials such as Inconel 825 and Incalloy. The units for the brine treatment section were mainly constructed from stainless steel 316. The material of construction has a high corrosion resistance under subcritical conditions and is commonly used for construction of process units for MSF and MED [30–32]. The most expensive unit was the fired heater with the separator being the second most expensive unit due to the material of construction and high design pressures. The total fixed capital investment was M$ 83–99, with the investment decreasing for higher feed concentrations. This is mainly due to the lower cost of the SC heater (less duty) required and gravity separator, even though two extra heat exchangers are required for the feed pre-heating section. Mickley [33] extensively investigated different ZLD schemes for different flows and feed concentrations. For schemes containing thermal brine concentrators and crystallisers, the investment cost was between M$ 16–18 (0.4 wt% feed) and M$ 22–28 (1.2 wt% feed) for a feed of 1 million gal/d (3785 m^3/d). The investment costs are lower; however, the cost does increase with feed concentration, which is not the case for SCWD. No pre-treatment costs were added for the schemes consisting of only thermal units. For the schemes containing a RO unit, as pre-concentration step, the cost of lime softener was added.

3.2. Brine treatment price

In order to estimate the brine treatment price, the annual capital and operating expenses were calculated. The annualised capital expense was calculated for an interest rate of 7% and for period of 25 years, which are typical values for a desalination plant [34,35]. The annual operating expenses consisted of the utilities, operations/labour and maintenance costs. As it was assumed that the SCWD unit would be added to an existing desalination facility, the expenses allotted for utilities and related facilities/plants such as electricity and steam generation were not considered. The utility costs included the cost of natural gas for the fired heater, electricity for the pump and the cooling water requirement to cool the dried NaCl stream to 50 °C. The detailed utility prices and annual utility cost can be found in the SI. The annual maintenance of SCWD unit was calculated to be 2% of the total fixed capital investment. This is typically done for membrane-based desalination plants, while for thermal desalination plants, such as MED, the maintenance is taken as 0.2% of the fixed capital [36]. However, due to the corrosive environment and extreme operating conditions a conservative maintenance estimate of 2% was taken rather than the conventional 0.2%. Further detailed information of the operating costs can be found in the SI. The cost of brine pre-treatment was not included in the operating costs as this is dependent on the brine source. For drinking water production, the brine stream is already pre-treated before desalination and minimal pre-treatment would be required. Brine produced during hydraulic fracturing would require extensive pre-treatment, which would increase the overall brine treatment price. This is discussed further in Section 3.3.

The income of the SCWD unit was calculated for the SCW, steam and NaCl production. The steam produced during brine expansion (235 °C and 22 bar), is partially used to pre-heat concentrated feeds. The remainder of the steam as well as the steam produced for the lower concentration feeds (3.5 and 7 wt%), was sold as MP steam utility. In Table 6, a summary of the annual expenses and income is given as well as the cost of brine treatment.

In Table 6, the brine treatment price is reported for an ideal case where all the products are sold and a more realistic case where none of the products are sold. The sale of the product is dependent on the quality of the products. For example, the MP steam could contain entrained salt particles which would lower the steam quality, making the direct use of the steam impossible. Demisters would have to be installed to prevent the entrainment, similar to what is done for MSF and MED. Alternatively, the heat of the steam could be used to generate high quality steam using a heat exchanger. Further analysis, on the effect of product sales, is shown in Section 3.2.1.1. It is seen that the feed concentration has a great effect on the brine treatment cost (Incl. income) decreasing the treatment cost with a factor ~ 8. This is partially due to the lower annual investment and operating expenses; however, the higher income of the salt is the main contributor to lowering the cost. This shows that the price of water alone is too low to make the process economically feasible and that other products, such as steam and salt, also need to be sold to cover the rest of the expenses. For the chosen separator conditions (430 °C and 270 bar), the total dissolved concentration (TDS) concentrations of the SCW phase was 680 ppm, which is below the limit for fresh drinking water (> 750 ppm TDS) [37]. However, as the brine fed system is a waste stream from another process, the water cannot be sold as drinking water. Therefore, the produced water can be used as process water (utility), for another section of the plant with which the SCWD unit would be integrated. In the case of hydraulic fracturing, the water can be recycled back to the wells.

The optimisation of the brine expansion and steam integration contributed to reduction in the brine treatment cost. For a feed of 20 wt % NaCl, the brine treatment price would be \$ 3.06/m^3_{brine} (~3 times higher compared to the current treatment price), due the additional utility expenses for MP steam.

Based on salt content of the feed, the cost ranges from \$ 321–40/tonne NaCl, if no salt were to be sold, showing that the process becomes cheaper for more salt in the feed. Compared to the cost of a spray dryer (\$ 90/t solid), the SCWD unit is more favourable for concentrated feeds [6].

3.2.1. Sensitivity analysis

3.2.1.1. Product income. Depending on the source of feed (brine) and the quality of the products (process water, MP steam and salt), some or all of the products might not be sold thereby affecting the brine treatment prices. In Fig. 9, a comparison is given, of the effect that the sale of each product has on the brine treatment price.

From the results it is seen that the loss of income from either MP steam or process water does not have a significant influence on the

Table 4
Feed and product rates of a SCWD unit for different feed concentrations (capacity of 5000 m^3/d).

	3.5	7.0	14	20
Feed (kton/year)	1687	1728	1814	1891
NaCl (kton/year)	58	120	253	378
Total water produced (kton/yr)	1629	1608	1561	1513
SCW water (kton/yr)	1534	1412	1148	898
Condensate (kton/yr)	48	99	207	308
MP steam (kton/yr)	47	97	206	307

Table 5
Summary of fixed SCWD capital investment (see Fig. 7) for different feed concentrations (wt% NaCl).

Unit	Material of construction	Design pressure (bar)	Design temperature (°C)	Estimation method	Capital investment (M$)			
					3.5	7.0	14	20
High-pressure pump	SS 316	300	50	Seider et al. [27]	2.24	2.29	2.41	2.51
SCW-feed pre-heat HEX	SS 316	300	210	Peters et al. [26]	–	–	0.73	1.10
Steam-feed pre-heat HEX	SS 316	300	210	Peters et al. [26]	–	–	0.03	0.18
SC HEX	Inconel 825 (tube) SS 316 (Shell)	300	460	Peters et al. [26]	2.05	2.05	2.05	2.05
SC heater	Incalloy (tubes)	300	460	Woods [29]	11.90	11.80	11.20	8.67
Separator	Inconel 825	300	460	Seider et al. [27]	6.58	6.09	4.77	4.11
1st flash	SS 316	44	290	Seider et al. [27]	0.03	0.07	0.17	0.39
2nd flash-evaporator	SS 316	24	290	Peters et al. [26]	0.30	0.21	0.33	0.42
Cooler	SS 316	24	290	Peters et al. [26]	0.01	0.01	0.01	0.01
Total fixed capital investment (Lang factor 4.28)					99	96	93	83

Table 6
Economic evaluation of SCWD unit for four different feed concentrations (plant capacity of 1650 000 m^3/yr with of 90% availability).

	Unit	3.5	7.0	14	20
Annualised capital cost[a]	M$/yr	8.50	8.27	7.97	7.14
Annual operating cost	M$/yr	10.12	9.97	9.53	7.84
Annual NaCl income[b]	M$/yr	(−1.74)	(−3.60)	(−7.60)	(−11.33)
Annual steam income[c]	M$/yr	(−0.49)	(−1.02)	(−1.64)	(−1.43)
Annual water income[d]	M$/yr	(−0.52)	(−0.48)	(−0.39)	(−0.31)
Brine treatment cost (Excl. income)[e]	$/$m^3$	11.28	11.06	10.60	9.08
Brine treatment cost (Incl. income)[e]	$/$m^3$	9.61	7.97	4.77	1.16
Cost based on salt (Excl. salt income)	$/tonne salt	321	152	69	40
Cost based on salt (Incl. salt income)	$/tonne salt	291	122	39	10

[a] $A = P\frac{[i(1+i)^n]}{[(1+i)^n-1]}$ compound interest formula.
[b] NaCl price $30/ton [14].
[c] MP steam (22 bar; 235 °C) price $ 10.5/ton [27].
[d] Process water price $ 0.34/m^3, only SCW is sold [27].
[e] Based on m^3 of brine fed.

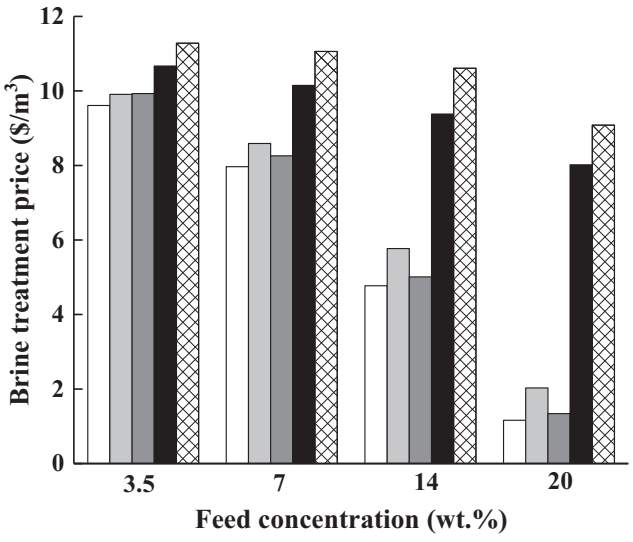

Fig. 9. Influence of product income on brine treatment price (□ – Ideal case ■ -No steam income; ■ - No water income; ■ – No salt income; pattern – No income).

brine treatment price, as these are low value products when compared to the salt. The loss of the salt income has the greatest influence on the brine treatment price, especially for higher concentration feeds for which more salt is produced. For a feed concentration of 20 wt%, the brine treatment price will increase from $ 1.16 to 7.98/m^3_{brine}. Thus, the sale of salt, even as a low-quality product, is important for making the SCWD more economically favourable, especially for concentrated waste brine streams.

3.2.1.2. Salt waste disposal. For the scenario where the salt is not sold as low-quality salt, it will have to be disposed of as non-hazardous solid waste, which in turn will increase the operating cost and brine treatment price. In Fig. 10, the effect of salt disposal costs on the brine treatment price is shown, assuming that the disposal cost of non-hazardous solid waste is $ 33/ton [38].

The results show that compared to the idealised case and the case where no income is considered, the brine treatment will increase considerably when the cost of waste disposal is also included. The SCWD process will become more expensive for higher concentration feeds. Even though, the annual capital and other operating expenses decrease with feed concentration, the cost of solid waste disposal is such that the annual operating expenses (and thereby the brine treatment price) increase significantly for higher concentration feeds. For a feed concentration of 20 wt%, the brine treatment price will increase to $ 16.60/m^3_{brine} (most waste is produced). For lower concentrations (3.5 and 7 wt% NaCl), the brine treatment price will be between $ 12–13/

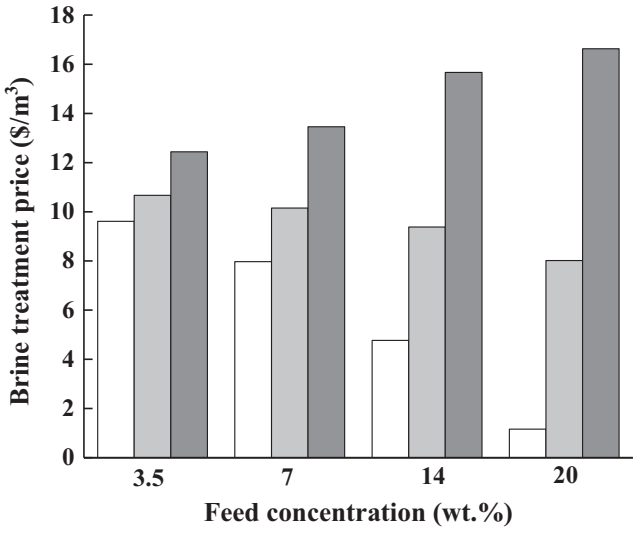

Fig. 10. Influence of salt sale and salt disposal cost on brine treatment price (□ – Ideal case ■ – No income; ■ – Salt disposal).

m^3_{brine}.

Even though the brine treatment price increases significantly it is still comparable with disposal techniques such as deep-well injection (when transportation costs are included) and lined evaporation ponds. In a review by Panagopoulus et al. [6], it is reported that the disposal cost was between \$ 3.28–10.04/m^3_{brine} for evaporation ponds and \$ 0.54–2.65/m^3_{brine} for deep-well injection (excluding the transportation costs). For a low concentration feeds (3.5 and 7 wt%), the SCWD brine treatment price is slightly higher than an expensive lined evaporation pond. Lokare et al. [39] reported that for deep-well injection (treatment of waste brine from hydraulic fracturing), transportation costs to the injection sites range between \$ 10–20/barrel (\$ 83–167/m^3), with the injection cost being \$ 1/barrel (\$ 8.3/m^3). Able & Trembly [40] also reported the values between \$ 4–8/barrel (\$ 34–67/m^3) for brine disposal and transportation costs of \$ 20/barrel (\$ 167/m^3). The SCWD brine treatment price, including solid waste disposal, is thus less expensive than deep-well injection, which is mainly due to the high transportation cost of the brine to the injection sites.

3.2.1.3. Natural gas price and brine inlet temperature. Next to the effect of the product income and solid waste disposal, the effect of the natural gas price and the feed inlet temperature was also examined. The results are shown in Fig. 11.

If the natural gas price was \$ 1.26/GJ [26] the treatment price for a 3.5 wt% feed would be \$ 7.06/$m^3_{brine,}$ which is still high compared to conventional desalination processes, while for 20 wt% (idealised case) the treatment price would become \$ −0.61/m^3_{brine}.

Fig. 11b shows the effect of the brine inlet temperature for a feed of 14 and 20 wt%. For the base case evaluation, it was assumed that the feed enters the SCWD unit at 25 °C and 1 bar for all feed concentrations. For thermal desalination plants the operating temperatures are in the range of 65–70 °C (MED) and 90–110 °C (MSF) and the brine waste has to be cooled before being disposed [25]. Regulations state that the brine waste discharge temperature should be a maximum of 10 °C higher than the seawater [6,7,25]. If, however, the concentrated waste brine was fed to a SCWD post-treatment unit, cooling is superfluous, as higher feed temperatures are beneficial for heat integration, especially for concentrated feeds [19]. For a feed of 14 and 20 wt%, higher temperatures would lead to less steam consumption (Steam-Feed pre-heat, Fig. 7) and more MP steam would be left to be sold as utility. If the inlet temperature is increased to 90 °C, the brine treatment cost (Incl. income) would reduce from \$ 4.77 to 4.50/m^3_{brine} for a 14 wt% feed and \$1.16 to 0.76/m^3_{brine} for a 20 wt% feed. The effect of the inlet temperature is greater for a 20 wt% feed, due to the higher steam production rate. For an inlet temperature of 110 °C, the treatment cost drops to \$ 0.64/m^3_{brine} (for 20 wt% feed). In addition to the increased sale of MP steam, the capital expenses for a 14 and 20 wt% would also decrease as a smaller or no Steam-Feed HEX would be required. However, this effect was not included in the analysis.

3.3. Comparison with other SCWD economic evaluations

The SCWD process is still an emerging desalination technology and the number of economic evaluations is limited. The group of Trembly have conducted a few studies, to evaluate the economic feasibility of the application of SCWD for the treatment of multi-component waste water streams produced during hydraulic fracturing [14,38,40].

Lopez & Trembly [14] simulated the SCWD process using Aspen Plus. A multi-component brine stream (15.5 wt% TDS) was treated at 221 bar and 430 °C. The estimated treatment cost of their SCWD process was \$ 4.29–7.10/m^3_{brine} (Incl. income). The minerals retrieved during the pre-treatment steps *i.e.* $BaSO_4$, $Mg(OH)_2$, $CaCO_3$ and $SrCO_3$ were sold at prices ranging from \$ 100–200/ton. The recovered NaCl from the separation was also sold at a price of \$ 30/ton. If, however, the minerals were not sold, the cost would be \$ 25/m^3_{brine}, which is higher than the treatment cost (Excl. income) reported in Table 6. The required chemicals for pre-treatment of the brine increased the operational expenses of their process, making the process more expensive in comparison to our proposed process.

Able & Trembly [40], performed an extensive economic evaluation using simulations and experimentally validated results. The default conditions were for a brine feed rate of 545 m^3/d (100 gpm) and inlet concentration of 17.6 wt% TDS. Separation occurred at 250 bar and the water recovery was set to 50% (mass basis). For the default conditions, two scenarios were investigated for ZLD. The first considered the disposal of the NaCl and KCl salts, and the cost of solid disposal was included in the operating cost (\$ 33/ton). The second scenario considered the sale of the salt as rock salts (\$ 72/ton). The cost of brine treatment for the disposal case was \$ 85/m^3_{brine} (\$10.19/barrel), while the cost for the salt income scenario was \$ 58/m^3_{brine} (\$6.89/barrel). The cost of both scenarios was much higher compared to the values presented in Figs. 9 and 10, which is mainly related to the costs associated with the pre-treatment of the brine. As for their previous study [14], the pre-treatment cost was included in the analysis. The cost for the chemicals required for pre-treatment of the feed was \$ 32/m^3_{brine} (\$ 3.78/barrel) and was the largest contribution to the brine treatment price. Apart from the pre-treatment costs, the cost of solid waste disposal was the biggest contributor. The contribution of the solid waste disposal, to the total brine treatment price was \$ 2.48/m^3_{brine} (\$ 0.28/barrel) for hazardous waste and \$ 7.55/m^3_{brine} (\$ 0.90/barrel) for non-hazardous

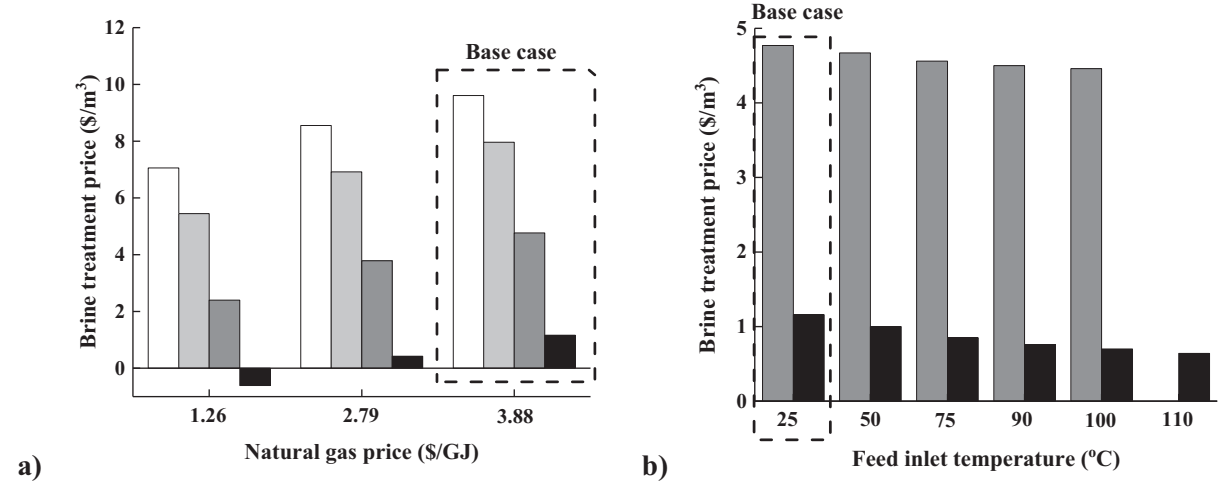

Fig. 11. Brine treatment price (idealised case) sensitivity analysis a) Natural gas price b) Feed inlet temperature (□ – 3.5 wt%; ■ – 7.0 wt%; ■ – 14 wt%; ■ – 20 wt%).

waste.

From the above comparison it can be concluded the source of the brine feed will have a great influence on the overall brine treatment price. For thermal desalination units, the cost of pre-treatment ranges between \$ 1.29–1.92/m^3_{brine}, (feed rate of 50–800 m^3/h) which would increase the treatment marginally [41]. However, for concentrated brines originating from wells and reservoirs, during processes such as hydraulic fracturing and CO_2 sequestration, the treatment price will increase significantly due to the extensive pre-treatment required.

4. Technology comparison and application

As mentioned in the Introduction, brine management and treatment are important aspects of desalination. This is mainly tied to the growing global desalination capacity and conversely the increase in brine production and discharge. Brine streams are not only linked to the production of fresh drinking water, but are also the side-products of hydraulic fracturing, CO_2 sequestration and obtained as waste streams of the dairy, textile and leather industry [2,5,14,42–46]. The development and implementation of ZLD technologies/processes is important for the reduction of brine waste [1,6–8,47]. ZLD is normally a three step process namely 1) pre-concentration of the brine, 2) brine concentration up to saturation and 3) crystallisation [6,8,33]. Pre-concentration is usually done using membranes. RO membranes are favourable for concentrating streams up to ~7 wt%, after which other technologies (mostly thermal-based) become more favourable. Other membrane processes such as ED, UF, NF, high pressure RO and membrane distillation (MD) (mix between membrane and thermal-based technologies) can also be used and are able to achieve higher outlet concentrations [6,7,33,48].

In order to concentrate the brine up to saturation, thermal-based methods are employed. These technologies include MSF, MED and MVC. Once the brine has been concentrated up to saturation, the last step is crystallisation, which is done using brine crystallisers, spray dryers and eutectic freeze crystallisers (emerging technology) [6–8,33]. Of the three ZLD steps, crystallisation is the most energy intensive, followed by the thermal brine concentration step. Compared to the pre-concentration step, the brine concentration step is a factor ~2 more energy intensive and crystallisation a factor ~4 [6].

In Fig. 12, the brine treatment prices of different desalination technologies, near-ZLD (brine concentrated up to saturation and then discharged) and complete ZLD processes are compared with the ideal brine treatment price for SCWD (all products are sold). For the comparison, only commercially available technologies were considered and not emerging technologies.

From the overview, it is seen that for low concentration feeds (3.5 and 7 wt%) the treatment cost of SCWD is expensive compared to other process. As the feed concentration increases up to 14 wt%, the process becomes comparable with other SCWD processes and near-ZLD technologies. For feed concentrations close to saturation (20 wt%), the ideal treatment price is comparable to that of thermal-based technologies. If the cost of solid waste disposal would be considered for the SCWD scheme, the brine treatment price for concentrated waste streams would increase considerably, but this would also be the case for the other units producing either a brine or solid waste. For the above comparison, some studies did not include the cost of pre-treatment or the disposal costs associated with the concentrated brine, while for other this was included. For a more thorough comparison, these costs should either be neglected or included for all studies.

In general, when comparing SCWD to conventional ZLD technologies, the advantages are 1) the unit is more compact, 2) the energy consumption of the unit decreases with feed concentration, and 3) it is versatile, in that it could be used for the treatment of mixed brine streams on the condition that VLE is formed under supercritical conditions [13].

SCWD is applicable to a wide range of feed concentrations, but is most appropriate (in terms of energy consumption and economics) for the treatment of high concentration brines. Specifically, SCWD would be best suited for smaller scale thermal desalination plants. The waste streams of these plants are more concentrated (7 wt% - saturation) and have higher discharge temperatures (30–45 °C), both factors that reduce energy consumption and treatment cost [6,50,51]. For these waste streams minimal pre-treatment is required and the brine treatment price will not increase considerably. Conversely, the SCWD could be used for the treatment of waste streams produced during hydraulic fracturing and CO_2 sequestration. The produced brine for both these processes vary in concentration depending on the reservoirs, but the average concentrations are between 15 and 18 wt%, with the maximum being 25–30 wt% [3,15,44,45,52]. The pre-treatment of the streams would, however, be required which will increase the brine treatment price considerably. The use of SCWD for the treatment of hydraulic fracturing waste has already been investigated to some extent [14,15,53].

Another consideration, for the application of SCWD, is the composition of the brine feed stream. For our proposed process it is important that VLE be established under supercritical conditions. This is usually the case for streams containing type I salts (*e.g.* NaCl, KCl, $CaCl_2$ and $MgCl_2$) or salt mixtures in which the type I salt is the major component. For type II systems (*e.g.* Na_2CO_3, Na_2SO_4 and K_2SO_4) a fluid-solid equilibria is formed, which would cause plugging and eventually lead to equipment failure [54,55]. For the above mentioned waste streams, the main salts present are NaCl and $CaCl_2$, which makes the separation under supercritical conditions easy, as a VLE system is obtained [15,44] even with certain concentration of type II salts present. The application of SCWD for multi-component feeds will be investigated in future work.

5. Conclusions

Detailed process calculations (using the AP EoS and eNRTL model) of the SCWD unit, were extended to the brine treatment section to maximise steam production and achieve ZLD. ZLD was achieved by a two stage expansion of the hydrothermal brine (remaining after separation of SCW), utilising the steam produced during the first stage flash to dry the salt in the second stage flash-evaporation. A window of operation (with the pressures of the two stages as variables) was established in which the brine treatment section could be operated to achieve ZLD. The optimum point of operation was located around the maximum second stage pressure, where the exergy of the second stage (flash-evaporation step) steam was also a maximum, due to the high pressure and corresponding temperature. Comparison of the theoretical

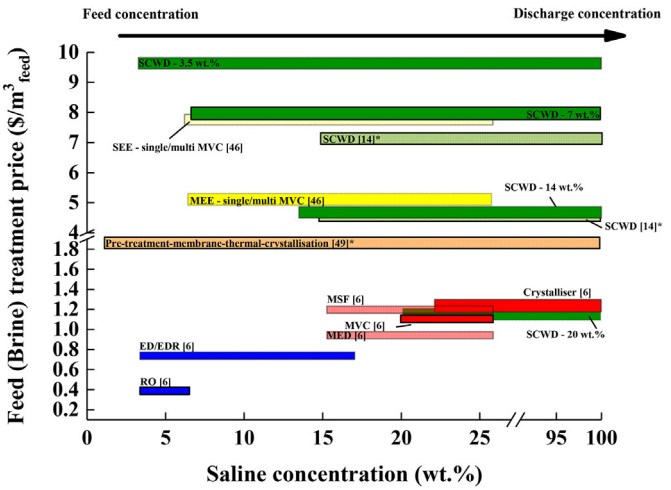

Fig. 12. Brine treatment price comparison for different desalination technologies (■ Membrane-based; ■ Thermal-based; ■ near-ZLD; ■ ZLD; ■ SCWD-ZLD) (* indicates that pre-treatment cost (chemicals) was included) [49].

and operational maximum pressures revealed that the values were in the same range and that optimum operating pressures could be determined from the theoretical pressures, as a first estimate. However, for more precise pressure values more extensive modelling and calculations were required.

Through optimisation of the brine recovery section, the energy consumption of the entire SCWD process, for concentrated feed streams, was reduced by using the generated steam to pre-heat the streams. For a 14 wt%, feed the total energy consumption reduced to 0.74 MJ_{th}/kg_{feed} (4% reduction) and for a 20 wt% feed, the energy consumption reduced to 0.54 MJ_{th}/kg_{feed} (24% reduction).

An economic analysis was done to determine the brine treatment price of SCWD unit (for four feed concentrations), for a general case in which the source of the brine feed is not specified, at a capacity of 5000 m^3_{feed}/d. The economic analysis showed that by increasing the feed concentration from 3.5 to 20 wt%, the brine treatment price decreased from $ 9.61 to 1.16/m^3_{brine}, for an ideal case where all the products (salt, steam and water) were sold. The income of the salt was the main contributor to making the SCWD economically favourable, as the steam and water income had a minimal effect on the brine treatment price. Apart from the income of the products, the brine treatment price also decreased with feed concentration due to the lower capital (smaller SC heater) and operating (lower energy consumption) expenses. For the case, where the salt was disposed as solid waste the brine treatment price increased considerably (> factor 10) for high concentration feeds. However, it was still lower than the price of deep-well injection (brine disposal method) which was due to the transportation costs associated with the disposal method.

Comparison with other SCWD economic evaluations, revealed that the brine treatment price greatly depends on the source of the brine feed and the extent of pre-treatment required. For brine streams coming from desalination plants, the brine treatment price would increase marginally. However, for brine waste streams originating from hydraulic fracturing the required pre-treatment was extensive and the brine treatment price would increase considerably, mainly due to the cost of pre-treatment chemicals and solid waste disposal.

The proposed SCWD process (idealised case) was comparable, with regards to the brine treatment price, to near-ZLD processes, other SCWD processes (salt income included) and thermal-based units, for high concentration feeds (14 and 20 wt% NaCl). It was recommended that SCWD be used for the treatment of concentrated waste brine streams of small capacity thermal desalination plants or other processes which produce concentrated waste streams at high outlet temperatures.

Author statement

Surika van Wyk: Conceptualization, Methodology, Software, Validation, Investigation: Writing – Original Draft, Writing – Review & Editing; Visualization **Aloijsius G. J. van der Ham:** Conceptualization, Supervision, Project administration, Funding acquisition **Sascha R. A. Kersten:** Conceptualization, Supervision, Project administration, Funding acquisition.

Declaration of competing interest statement

We the authors that we have no significant competing financial, professional, or personal interests that might have influenced the performance or presentation of the work described in this manuscript.

Acknowledgements

This work was performed in the cooperative framework of Wetsus, European Centre of Excellence for Sustainable Water Technology (www.wetsus.nl). Wetsus is co-funded by the Dutch Ministry of Economic Affairs and Ministry of Infrastructure and Environment, the European Union Regional Development Fund, the Province of Fryslân and the Northern Netherlands Provinces. This work is part of a project that has received funding from the European Union's Horizon 2020 research and innovation programme under the Marie Skłodowska-Curie grant agreement No 665874. The authors would like to thank the participants of the research theme “Desalination” for the fruitful discussions and their financial support.

Appendix A. Supplementary data

Supplementary data to this article can be found online at https://doi.org/10.1016/j.desal.2020.114593.

References

[1] E. Jones, M. Qadir, M.T.H. van Vliet, V. Smakhtin, S. mu Kang, The state of desalination and brine production: a global outlook, Sci. Total Environ. 657 (2019) 1343–1356, https://doi.org/10.1016/j.scitotenv.2018.12.076.
[2] O. Lefebvre, R. Moletta, Treatment of organic pollution in industrial saline wastewater: a literature review, Water Res. 40 (2006) 3671–3682, https://doi.org/10.1016/j.watres.2006.08.027.
[3] R.J. Klapperich, G. Liu, D.J. Stepan, M.D. Jensen, D. Charles, E.N. Steadman, J.A. Harju, D.V. Nakles, IEAGHG investigation of extracted water from CO 2 storage : potential benefits of water extraction and lesson learned, Energy Procedia 63 (2014) 7173–7186, https://doi.org/10.1016/j.egypro.2014.11.753.
[4] C.E. Clark, J.A. Veil, Produced Water Volumes and Management Practices in the United States, Argonne National Laboratory, 2009.
[5] H.M. Breunig, J.T. Birkholzer, A. Borgia, C.M. Oldenburg, P.N. Price, T.E. McKone, Regional evaluation of brine management for geologic carbon sequestration, Int. J. Greenh. Gas Control. 14 (2013) 39–48, https://doi.org/10.1016/j.ijggc.2013.01.003.
[6] A. Panagopoulos, K. Haralambous, M. Loizidou, Desalination brine disposal methods and treatment technologies - a review, Sci. Total Environ. 693 (2019) 133545, https://doi.org/10.1016/j.scitotenv.2019.07.351.
[7] T. Tong, M. Elimelech, The global rise of zero liquid discharge for wastewater management: drivers, technologies, and future directions, Environ. Sci. Technol. 50 (2016) 6846–6855, https://doi.org/10.1021/acs.est.6b01000.
[8] A. Giwa, V. Dufour, F. Al Marzooqi, M. Al Kaabi, S.W. Hasan, Brine management methods: recent innovations and current status, Desalination. 407 (2017) 1–23, https://doi.org/10.1016/j.desal.2016.12.008.
[9] H.W. Chung, K.G. Nayar, J. Swaminathan, K.M. Chehayeb, J.H. Lienhard V, Thermodynamic analysis of brine management methods: Zero-discharge desalination and salinity-gradient power production, Desalination 404 (2017) 291–303, https://doi.org/10.1016/j.desal.2016.11.022.
[10] G.P. Thiel, E.W. Tow, L.D. Banchik, H.W. Chung, J.H. Lienhard V, Energy consumption in desalinating produced water from shale oil and gas extraction, Desalination 366 (2015) 94–112, https://doi.org/10.1016/j.desal.2014.12.038.
[11] A.H. Harvey, D.G. Friend, Physical properties of water, in: Donald A. Palmer, R.J. Fernández-Prini, A.H. Harvey, 1ste ed. (Eds.), Aqueous Syst. Elev. Temp. Press. Phys. Chem. Water,Steam Hydrothermal Solut. Elsevier Academic Press, Amsterdam, 2004, pp. 1–27.
[12] S.O. Odu, A.G.J. Van Der Ham, S. Metz, S.R.A. Kersten, Design of a Process for supercritical water desalination with zero liquid discharge, Ind. Eng. Chem. Res. 54 (2015) 5527–5535, https://doi.org/10.1021/acs.iecr.5b00826.
[13] S. van Wyk, S.O. Odu, A.G.J. van der Ham, S.R.A. Kersten, Design and results of a first generation pilot plant for supercritical water desalination (SCWD), Desalination 439 (2018), https://doi.org/10.1016/j.desal.2018.03.028.
[14] D.E. López, J.P. Trembly, Desalination of hypersaline brines with joule-heating and chemical pre-treatment: conceptual design and economics, Desalination. 415 (2017) 49–57, https://doi.org/10.1016/j.desal.2017.04.003.
[15] D.D. Ogden, J.P. Trembly, Desalination of hypersaline brines via joule-heating: experimental investigations and comparison of results to existing models, Desalination. 424 (2017) 149–158, https://doi.org/10.1016/j.desal.2017.10.006.
[16] C.M. Able, D.D. Ogden, J.P. Trembly, Sustainable management of hypersaline brine waste: zero liquid discharge via joule-heating at supercritical condition, Desalination. 444 (2018) 84–93, https://doi.org/10.1016/j.desal.2018.07.014.
[17] D. Xevgenos, K. Moustakas, D. Malamis, M. Loizidou, An overview on desalination & sustainability: renewable energy-driven desalination and brine management, Desalin. Water Treat. 57 (2016) 2304–2314, https://doi.org/10.1080/19443994.2014.984927.
[18] V.G. Gude, Energy storage for desalination processes powered by renewable energy and waste heat sources, Appl. Energy 137 (2015) 877–898, https://doi.org/10.1016/j.apenergy.2014.06.061.
[19] S. van Wyk, A.G.J. van der Ham, S.R.A. Kersten, Analysis of the energy consumption of supercritical water desalination (SCWD), Desalination. 474 (2020) 114189, https://doi.org/10.1016/j.desal.2019.114189.
[20] A. Anderko, K.S. Pitzer, Equation-of-state representation of phase equilibria and volumetric properties of the system NaCl-H2O above 573 K, Geochim. Cosmochim. Acta 57 (1993) 1657–1680, https://doi.org/10.1016/0016-7037(93)90105-6.
[21] J.J. Kosinski, A. Anderko, Equation of state for high-temperature aqueous electrolyte and nonelectrolyte systems, Fluid Phase Equilib. 183–184 (2000) 75–86, https://doi.org/10.1016/S0378-3812(01)00422-8.

[22] Y. Song, C.-C. Chen, Symmetric Electrolyte Nonrandom Two-Liquid Activity Coefficient Model, Ind. Eng. Chem. Res. 48 (2009) 7788–7797, https://doi.org/10.1021/ie9004578.
[23] Y. Yan, C.C. Chen, Thermodynamic representation of the NaCl + Na2SO4 + H2O system with electrolyte NRTL model, Fluid Phase Equilib. 306 (2011) 149–161, https://doi.org/10.1016/j.fluid.2011.03.023.
[24] I.C. Karagiannis, P.G. Soldatos, Water desalination cost literature: review and assessment, Desalination. 223 (2008) 448–456, https://doi.org/10.1016/j.desal.2007.02.071.
[25] M.W. Shahzad, M. Burhan, L. Ang, K.C. Ng, Energy-water-environment nexus underpinning future desalination sustainability, Desalination. 413 (2017) 52–64, https://doi.org/10.1016/j.desal.2017.03.009.
[26] M.S. Peters, K.D. Timmerhaus, R.E. West, Plant Design and Economics for Chemical Engineers, Fifth, McGraw-Hill, Singapore, 2004.
[27] W.D. Seider, J.D. Seader, D.R. Lewin, S. Widagdo, 3rd ed. (Ed.), Product and Process Design Principles: Synthesis, Analysis, and Evaluation, John Wiley & Sons, 2010.
[28] S. Jenkins, Chemical engineering plan cost index: 2018 annual value, Chem. Eng. (2019), www.chemengonline.com/2019-cepci-updates-january-prelim-and-december-2018-final/ , Accessed date: 30 March 2019.
[29] D.R. Woods, Rules of Thumb in Engineering Practice, Wiley-VCH Verlag & Co. KGaA, Darmstadt, 2007.
[30] P. Boillot, J. Peultier, Use of stainless steels in the industry : recent and future developments, Procedia Eng. 83 (2014) 309–321, https://doi.org/10.1016/j.proeng.2014.09.015.
[31] J.W. Oldfield, B. Todd, Technical and economic aspects of stainless steels in MSF desalination plants, Desalination. 124 (1999) 75–84, https://doi.org/10.1016/S0011-9164(99)00090-9.
[32] M.A. Deyab, Enhancement of corrosion resistance in MSF desalination plants during acid cleaning operation by cationic surfactant, Desalination. 456 (2019) 32–37, https://doi.org/10.1016/j.desal.2019.01.018.
[33] M. Mickley, Survey of High-Recovery and Zero Liquid Discharge Technologies for Water Utilities, (2008).
[34] S. Al-Obaidani, E. Curcio, F. Macedonio, G. Di Profio, H. Al-Hinai, E. Drioli, Potential of membrane distillation in seawater desalination: thermal efficiency, sensitivity study and cost estimation, J. Memb. Sci. 323 (2008) 85–98, https://doi.org/10.1016/j.memsci.2008.06.006.
[35] G. Filippini, M.A. Al-Obaidi, F. Manenti, I.M. Mujtaba, Design and economic evaluation of solar-powered hybrid multi effect and reverse osmosis system for seawater desalination, Desalination. 465 (2019) 114–125, https://doi.org/10.1016/j.desal.2019.04.016.
[36] G. Filippini, F. Manenti, I.M. Mujtaba, Cost evaluation and optimisation of hybrid multi effect distillation and reverse osmosis system for seawater desalination, Desalination. 456 (2019) 136–149, https://doi.org/10.1016/j.desal.2019.01.019.
[37] UNESCO-WWAP, Water for People, Water for Life, http://www.unesco.org/new/en/natural-sciences/environment/water/wwap/wwdr/wwdr1-2003/, 2003.
[38] X. Dong, J. Trembly, D. Bayless, Techno-economic analysis of hydraulic fracking fl owback and produced water treatment in supercritical water reactor, Energy. 133 (2017) 777–783, https://doi.org/10.1016/j.energy.2017.05.078.
[39] O.R. Lokare, S. Tavakkoli, G. Rodriguez, V. Khanna, R.D. Vidic, Integrating membrane distillation with waste heat from natural gas compressor stations for produced water treatment in Pennsylvania, Desalination. 413 (2017) 144–153, https://doi.org/10.1016/j.desal.2017.03.022.
[40] C.M. Able, J.P. Trembly, Advanced supercritical water-based process concepts for treatment and bene fi cial reuse of brine in oil/gas production, Desalination. 481 (2020) 114334, https://doi.org/10.1016/j.desal.2020.114334.
[41] F. Mansour, S.Y. Alnouri, M. Al-Hindi, F. Azizi, P. Linke, Screening and cost assessment strategies for end-of-pipe zero liquid discharge systems, J. Clean. Prod. 179 (2018) 460–477, https://doi.org/10.1016/j.jclepro.2018.01.064.
[42] K. Kezia, J. Lee, B. Zisu, M. Weeks, G. Chen, S. Gras, S. Kentish, Crystallisation of minerals from concentrated saline dairy effluent, Water Res. 101 (2016) 300–308, https://doi.org/10.1016/j.watres.2016.05.074.
[43] T.A. Buscheck, J.M. Bielicki, J.A. White, Y. Sun, Y. Hao, W.L. Bourcier, S.A. Carroll, R.D. Aines, Pre-injection brine production in CO2 storage reservoirs: an approach to augment the development, operation, and performance of CCS while generating water, Int. J. Greenh. Gas Control. 54 (2016) 499–512, https://doi.org/10.1016/j.ijggc.2016.04.018.
[44] R. Kaplan, D. Mamrosh, H.H. Salih, S.A. Dastgheib, Assessment of desalination technologies for treatment of a highly saline brine from a potential CO2 storage site, Desalination. 404 (2017) 87–101, https://doi.org/10.1016/j.desal.2016.11.018.
[45] A. Carrero-parreño, V.C. Onishi, R. Ruiz-femenia, R. Salcedo-díaz, Optimization of multistage membrane distillation system for treating shale gas produced water, Desalination. 460 (2019) 15–27, https://doi.org/10.1016/j.desal.2019.03.002.
[46] V.C. Onishi, A. Carrero-parreño, J.A. Reyes-labarta, R. Ruiz-femenia, R. Salcedo-díaz, E.S. Fraga, J.A. Caballero, Shale gas flowback water desalination : single vs multiple-effect evaporation with vapor recompression cycle and thermal integration, Desalination 404 (2017) 230–248, https://doi.org/10.1016/j.desal.2016.11.003.
[47] S. Miller, H. Shemer, R. Semiat, Energy and environmental issues in desalination, Desalination. 366 (2014) 2–8, https://doi.org/10.1016/j.desal.2014.11.034.
[48] M. Turek, Dual-purpose desalination-salt production electrodialysis, Desalination. 153 (2003) 377–381, https://doi.org/10.1016/S0011-9164(02)01131-1.
[49] E. El Cham, S. Alnouri, F. Mansour, M. Al-Hindi, Design of end-of-pipe zero liquid discharge systems under variable operating parameters, J. Clean. Prod. 119569 (2019), https://doi.org/10.1016/j.jclepro.2019.119569.
[50] G. Filippini, M.A. Al-Obaidi, F. Manenti, I.M. Mujtaba, Performance analysis of hybrid system of multi effect distillation and reverse osmosis for seawater desalination via modelling and simulation, Desalination. 448 (2018) 21–35, https://doi.org/10.1016/j.desal.2018.09.010.
[51] P. Palenzuela, A.S. Hassan, G. Zaragoza, D.C. Alarcón-Padilla, Steady state model for multi-effect distillation case study: Plataforma Solar de Almería MED pilot plant, Desalination. 337 (2014) 31–42, https://doi.org/10.1016/j.desal.2013.12.029.
[52] K. Hunter, J.M. Bielicki, R. Middleton, P. Stauffer, R. Pawar, D. Harp, D. Martinez, Integrated CO2 storage and brine extraction, Energy Procedia 114 (2017) 6331–6336, https://doi.org/10.1016/j.egypro.2017.03.1769.
[53] S.A. Dastgheib, H.H. Salih, Treatment of Highly Saline Brines by Supercritical Precipitation Followed by Supercritical Membrane Separation, Ind. Eng. Chem. Res. 58 (2019) 3370–3376, https://doi.org/10.1021/acs.iecr.8b06298.
[54] V.M. Valyashko, Phase equilibria of water-salt systems at high temperatures and pressures, in: D.A. Palmer, R.J. Fernández-Prini, A.H. Harvey (Eds.), Aqueous Syst. Elev. Temp. Press. - Phyiscal Chem. Water, Steam Hydrothermal Solut, Elsevier Academic Press, Amsterdam, 2004, pp. 597–641, , https://doi.org/10.1016/B978-012544461-3/50016-8.
[55] M.M. Dipippo, K. Sako, J.W. Tester, Ternary phase equilibria for the sodium chloride–sodium sulfate–water system at 200 and 250 bar up to 400 °C, Fluid Phase Equilib. 157 (1999) 229–255, https://doi.org/10.1016/S0378-3812(99)00039-4.